Amyloid fibril formation by an SH3 domain

J. Iñaki Guijarro*, Margaret Sunde*, Jonathan A. Jones*, Iain D. Campbell[†], and Christopher M. Dobson*[‡]

Oxford Centre for Molecular Sciences, *New Chemistry Laboratory and [†]Department of Biochemistry, University of Oxford, South Parks Road, Oxford OX1 3QT, United Kingdom

ABSTRACT The SH3 domain is a well characterized small protein module with a simple fold found in many proteins. At acid pH, the SH3 domain (PI3-SH3) of the p85α subunit of bovine phosphatidylinositol 3-kinase slowly forms a gel that consists of typical amyloid fibrils as assessed by electron microscopy, a Congo red binding assay, and x-ray fiber diffraction. The soluble form of PI3-SH3 at acid pH (the A state by a variety of techniques) from which fibrils are generated has been characterized. Circular dichroism in the far- and near-UV regions and ^{1}H NMR indicate that the A state is substantially unfolded relative to the native protein at neutral pH. NMR diffusion measurements indicate, however, that the effective hydrodynamic radius of the A state is only 23% higher than that of the native protein and is 20% lower than that of the protein denatured in 3.5 M guanidinium chloride. In addition, the A state binds the hydrophobic dye 1-anilinonaphthalene-8-sulfonic acid, which suggests that SH3 in this state has a partially formed hydrophobic core. These results indicate that the A state is partially folded and support the hypothesis that partially folded states formed in solution are precursors of amyloid deposition. Moreover, that this domain aggregates into amyloid fibrils suggests that the potential for amyloid deposition may be a common property of proteins, and not only of a few proteins associated with disease.

The amyloidoses are a group of protein misfolding disorders characterized by the accumulation of insoluble fibrillar protein material in extracellular spaces (1, 2). The deposition of normally soluble proteins in this insoluble form is believed to lead to tissue malfunction and cell death. At least 16 different proteins and polypeptides have been identified in amyloid deposits to date. These include the Aβ peptide in Alzheimer's disease, the prion protein in the transmissible spongiform encephalopathies, the islet-associated polypeptide in type II diabetes, and other variant, truncated, or misprocessed proteins in the systemic amyloidoses (1, 2).

Proteins known to form amyloid fibrils *in vivo* have no obvious sequence or structural similarities, and where the soluble folds of the amyloidogenic precursors are known they span the range of secondary, tertiary, and quaternary structural elements. In spite of this diversity, there is a body of evidence that indicates that all amyloid fibrils have a common core structure (3). All amyloid fibrils are long, straight, and unbranching, with a diameter of 70–120 Å, and they all exhibit a cross-β diffraction pattern. Recent high-resolution fiber diffraction studies of different amyloid fibrils have shown a detailed molecular similarity at the level of the protofilament skeleton. The model initially proposed for the core structure of the transthyretin amyloid (4), which is a continuous β-sheet

helix, can be extended to other amyloids formed by proteins as diverse as lysozyme and Ig light chain (5).

The mechanism by which amyloidogenic proteins undergo the conversion from a soluble globular form to the cross-β conformation displayed by the disease-associated fibrils has not yet been elucidated. Nevertheless, the conformational reorganization associated with amyloid formation is well documented (6). Recent studies of some of the amyloidogenic variants of transthyretin (7), lysozyme (8), and the Ig light chain (9, 10) have started to investigate the process of conformational change that leads to amyloid deposition. Amyloid formation for the latter three proteins appears to start from partially structured forms of the proteins. The similar features displayed by all amyloid fibrils, regardless of their source, suggest that at least some elements of this process may be common to all amyloidogenic proteins. Here we report the *in vitro* formation of amyloid fibrils by the isolated, acid-denatured, SH3 domain from the p85α subunit of bovine phosphatidylinositol 3-kinase (PI3-SH3) and describe the characterization of the soluble amyloidogenic species from which SH3 fibril deposition occurs.

The SH3 domain (60–85 residues) is a small protein module that mediates specific protein–protein interactions within the cell (11, 12). The structure of PI3-SH3 (84 residues) is a β-barrel composed of two perpendicular, antiparallel β-sheets of three and two strands, respectively (13–15). The protein lacks disulfide bridges. Chemically denatured and unfolded states of the homologous drk SH3 domain in the absence of denaturant have been previously characterized (16–18). The refolding of chemically denatured PI3-SH3 has been investigated previously at neutral pH, and it has been shown that, like other SH3 domains (19–21), the protein folds cooperatively with no significant accumulation of intermediates (22). The folding/unfolding transition at neutral pH is reversible, and no evidence of aggregation was observed (22). At acid pH, a soluble form of the protein (A state) slowly aggregates and forms a gel that, as we show in this manuscript, consists of amyloid fibrils.

MATERIALS AND METHODS

Protein Preparation. The PI3-SH3 domain was expressed in *Escherichia coli* (strain BL21) as a fusion protein with glutathione *S*-transferase, purified, and lyophilized as previously described (13, 22). The original construct was kindly supplied by the Ludwig Institute, London. The recombinant protein used in this study consists of 84 residues from the SH3 domain of phosphatiidylinositol 3-kinase, plus a two-residue (GS) N-terminal extension and a four-residue (WNSS) C-terminal extension (22). SDS/PAGE, mass spectrometry, and N-

terminal sequencing analyses showed that the protein was pure and the molecular weight was that expected from the sequence.

Native protein (N state) samples were prepared by dissolving lyophilized PI3-SH3 in buffer 1 (20 mM NaH_2PO_4, pH 7.2). PI3-SH3 was denatured (D state) in 3.5 M guanidinium chloride solutions (GuHCl) prepared in buffer 1. This concentration of GuHCl is sufficient to denature fully PI3-SH3 for which the GuHCl concentration at the denaturation midpoint is 1.45 M at 20°C (22). Samples at pH 2.0 (A state) were obtained either by a pH jump from pH 7.2 samples or by directly dissolving lyophilized PI3-SH3 in buffer 1 after adjusting the pH to a value of 2.0 (buffer 2). Buffers were prepared either in H_2O or D_2O; pH measurements are uncorrected meter readings.

Fibril samples were obtained by incubating PI3-SH3 (10 mg/ml) in buffer 2 (pH 2.0) at room temperature or at 4°C for several days. Fibrils were formed (as judged by electron microscopy and/or Congo red binding) both when samples were prepared by dissolving lyophilized PI3-SH3 in buffer 2 and from solutions generated by dilution into this buffer from stock solutions at pH 7.2.

Congo Red Staining. Samples were tested for amyloid-specific Congo red binding by the spectroscopic band-shift assay described by Klunk *et al.* (23). A decapeptide with the sequence of the A-strand of transthyretin (residues 10–19), which forms amyloid fibrils spontaneously when dissolved in H_2O, was used as a positive control for amyloid. Aliquots of 10 mg/ml protein or peptide samples (10 μl) were diluted in the reaction buffer (5 mM sodium phosphate/150 mM NaCl, pH 7.4), which contained 5 μM Congo red (1 ml final reaction volume). The Congo red solution was freshly prepared and filtered through a 0.2 μm filter before use. The reaction samples were thoroughly mixed and incubated at room temperature for at least 30 min before recording the absorbance spectrum.

Electron Microscopy. Suspensions of PI3-SH3 fibrils were applied to Formvar-coated copper grids, blotted, negatively stained with 1% phosphotungstic acid (wt/vol), washed, air-dried, and then examined in a JEOL JEM1010 transmission electron microscope operating at an accelerating voltage of 80 kV.

X-Ray Diffraction. Fiber diffraction images were collected on a Cu K_α rotating anode equipped with a 180-mm MAR-Research Image plate (MAR Research, Hamburg, Germany) in the Laboratory of Molecular Biophysics, University of Oxford. Fibril samples were prepared by air-drying PI3-SH3 solutions (10 mg/ml initial concentration) between two wax-filled capillary ends. The distance between the capillaries was increased slowly, in small increments, to facilitate the alignment of the fibrils while drying occurred. This procedure produced a small stalk of fibrils protruding from the end of one of the capillaries, which was aligned in the x-ray beam. The fibril images were analyzed by using the display program IPDISP run on a Digital workstation (Digital Equipment Corporation, Maynard, MA).

NMR Spectroscopy. NMR experiments were recorded at 20°C by using a home-built NMR spectrometer operating at a proton frequency of 600.2 MHz and processed using FELIX 2.3 (Biosym Technologies, San Diego). One-dimensional ^1H spectra of the N, A, and D states were acquired with a spectral width of 8,000 Hz and a relaxation delay of 2.5 s.

Diffusion coefficients for the three states (N, A, and D) were determined by pulse field-gradient spin-echo NMR (24) by using the PG-SLED pulse sequence (25). Experiments were carried out by using buffers prepared in D_2O. A small quantity of dioxane was added to each sample as a radius standard (26), allowing changes in effective hydrodynamic radii to be determined. Data were fitted with KALEIDAGRAPH (Albeck Software, Reading, PA).

Circular Dichroism. Circular dichroism (CD) spectra in the near-UV and far-UV regions were obtained by using a Jasco J-720 spectropolarimeter equipped with a water bath to control the temperature at 20°C. Spectra were recorded for samples of the native protein at pH 7.2, the protein at pH 2.0, and the denatured protein in 3.5 M GuHCl. The pH 2.0 protein samples were freshly prepared and centrifuged to eliminate any possible large aggregate before CD experiments. The concentration of PI3-SH3 was 0.8 mg/ml for the near-UV measurements and 0.18 mg/ml for the far-UV experiments. Ten accumulations were averaged to obtain each spectrum. Cells with path lengths of 1 and 0.1 cm were used for near- and far-UV data acquisition, respectively.

ANS Binding. The fluorescence emission spectra of ANS (1-anilinonaphthalene-8-sulfonic acid) with and without protein were recorded on a Perkin–Elmer LS 50B spectrometer at 20°C. Protein samples (150 μM) in buffer 1 (pH 7.2), buffer 2 (pH 2.0), or in 3.5 M GuHCl were diluted 10-fold into the corresponding buffer containing ANS (250 μM final concentration). Samples were equilibrated for at least 15 min at 20°C before acquiring the fluorescence spectra.

RESULTS AND DISCUSSION

PI3-SH3 Fibril Characterization. PI3-SH3 incubated at pH 2.0 (in buffer 2) either at room temperature or at 4°C for periods ranging from several hours to several days slowly forms a translucent gel. Examination of the gel under the electron microscope showed fibrils that were tested for the three hallmarks of amyloid: staining with Congo red, a characteristic unbranched fibrillar appearance in the electron microscope, and a cross-β x-ray fiber diffraction pattern.

The PI3-SH3 fibrils show a red-shift in the Congo red solution assay, which is characteristic of amyloid fibrils (23). Congo red incubated in buffer alone shows a λ_{max} at 486 nm. Suspensions of PI3-SH3 fibrils show a relatively broad λ_{max} centered at 508 nm, and the point of maximal spectral difference between the fibril-containing solutions and dye-only solution occurs at 541 nm. Effectively identical λ_{max} (510 nm) and maximal spectral difference wavelength (541 nm) are displayed by the transthyretin peptide fibrils, which are known to be typical amyloid (5).

All known amyloid fibrils, regardless of the nature of the main protein component or the source of the fibrils, are between 70 and 120 Å wide and have no branch points. In the electron microscope the PI3-SH3 fibrils display typical amyloid morphology, appear very long, straight, and unbranching, and have a diameter of approximately 100 Å (Fig. 1). They show a distinct, twisting repeat which is similar to that observed in some preparations of Alzheimer amyloid peptides (27). Despite careful examination, no nonfibrillar, nonspecific aggregate was detected in the electron microscope preparations, suggesting that at pH 2.0 most if not all of the protein that aggregates forms amyloid fibrils.

The x-ray diffraction pattern exhibited by the PI3-SH3 fibrils (Fig. 2) contains two major reflections. Both of the reflections appear as rings because of the lack of relative fibril orientation within the sample. The dominant reflection is sharp and intense and occurs at 4.71 Å. A weaker and more diffuse reflection, centered at 9.42 Å but with the extremes of the reflection measured at 8.56 and 10.77 Å, is also visible. These two reflections constitute the cross-β pattern that is typical of amyloid diffraction and that is consistent with a core structure of β-sheet, in which the constituent β-strands lie at right angles to the long fiber axis. In well oriented fibril samples the reflections appear as arcs, rather than rings, and have distinguishing positions: the 4.7-Å reflection lies on the meridian and the 8- to 11-Å reflection lies on the equator. The 4.7-Å reflection arises from the interstrand spacing between β-strands in a β-sheet, in the direction of hydrogen bonding,
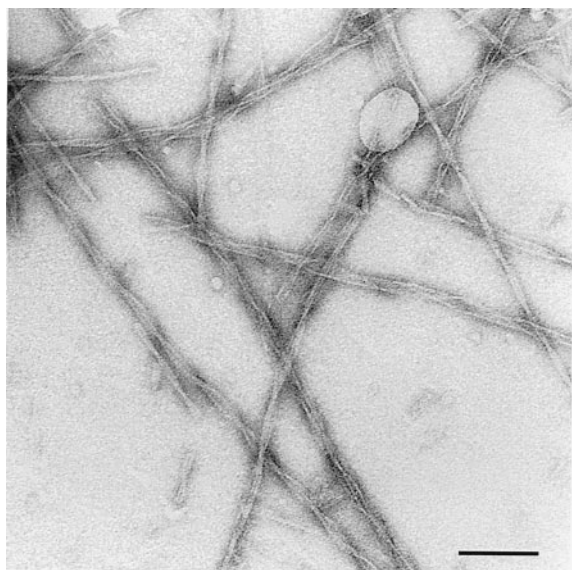
FIG. 1.   Electron micrograph of a negatively stained preparation of PI3-SH3 fibrils at pH 2.0. (Bar = 1,000 Å.)

and the 8- to 11-Å reflection corresponds to the intersheet spacing (see ref. 3 and references therein). In all amyloid samples the interstrand reflection is strong and relatively sharp for several reasons: there is only a small variation in the distance between strands in a β-sheet; this spacing is sequence-independent; and the hydrogen bonding extends along the length of the fibril for many hundreds of Å. The intersheet reflection is weaker and broader because the corresponding spacing is sequence-dependent and, therefore, variable, and because the fibrils are rotationally averaged around the long axis in the sample.

Characterization of the Soluble A State. The soluble A state, from which PI3-SH3 amyloid fibrils form, has been studied by NMR, CD, and an ANS-binding assay. Amyloid fibrils were generated from the A state samples whether these were prepared by a pH jump from neutral pH or by directly

dissolving PI3-SH3 in buffer 2 (pH 2.0), suggesting that fibril formation is due to conformers present at equilibrium at pH 2.0. The majority of the protein molecules in solution at pH 2.0 aggregated into the fibril-comprising gel as judged by the decrease in intensity of the signals in one-dimensional NMR spectra. The rate of formation of the gel was found to be concentration-dependent and varied between different sample preparations, with gel formation times ranging from several hours to several days. Experiments with the A state reported here were performed in a time frame in which no precipitation or gel formation was observed. Therefore, the data presented below reflect the properties of the soluble A state.

The one-dimensional NMR spectrum of the A state (Fig. 3*b*) shows a considerable loss of chemical shift dispersion relative to the spectrum of the native protein (Fig. 3*c*) and resembles the spectrum of the denatured protein in 3.5 M GuHCl (D state) (Fig. 3*a*). In particular, the native protein signals resonating at high field (0–0.6 ppm) are absent in the spectrum of the A state. These data indicate that the A state is substantially disordered relative to the native protein.

The relative effective hydrodynamic radii of the N, A, and D states of PI3-SH3 were determined from NMR diffusion experiments (Fig. 4). The effective radii of the A state and of the D state are, respectively, 23% (± 1%) and 48% (± 1%) larger than that of the native protein. Therefore, the A state is more compact than the protein denatured in 3.5 M GuHCl, which indicates that a substantial number of the conformers that constitute the A state are collapsed and, hence, partly folded. Substantial residual structure in an unfolded form of the homologous drk SH3 domain in the absence of denaturant has been reported previously (16–18).

The increase in effective radius of PI3-SH3 in the A state relative to the N state could be due to unfolding or oligomerization phenomena. Because NMR, CD, and fluorescence measurements (see below) indicate that the A state is less well organized than the N state, we conclude that the increase in effective radius of the A state is caused by an unfolding of the protein and that the A state is essentially monomeric. Other lines of evidence also suggest that the A state is essentially monomeric under the conditions studied here: diffusion rates
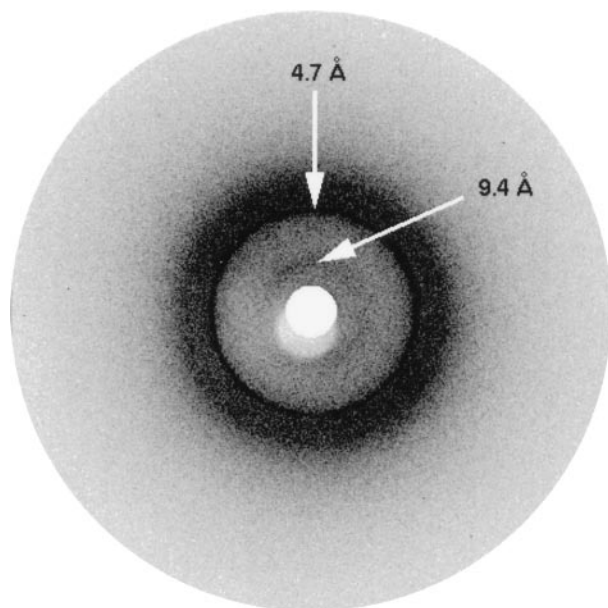

FIG. 2.   X-ray diffraction pattern of PI3-SH3 fibrils. The reflections generated by the interstrand spacing (4.7 Å) and the intersheet spacing (centered at 9.4 Å) typical of amyloid fibrils are marked by arrows. Because of poor alignment of the fibrils, these reflections appear as rings and do not display a meridional or equatorial character.
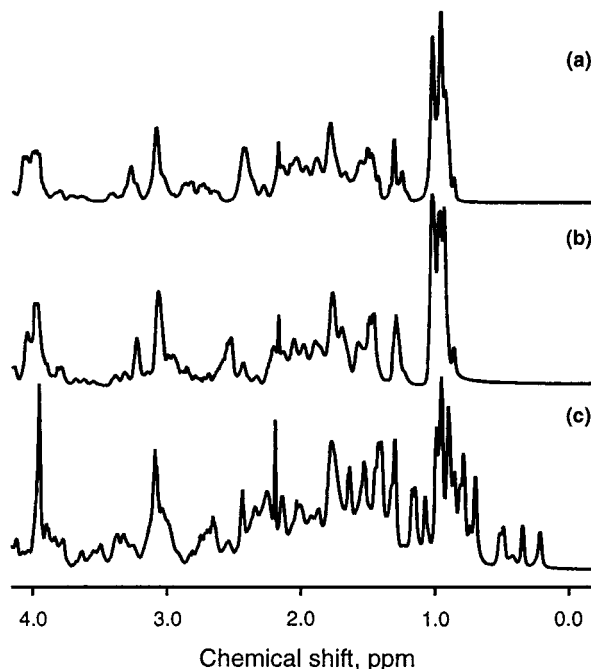

FIG. 3.   One-dimensional NMR spectra of the denatured protein (D) in 3.5 M GuHCl, pH 7.2 (*a*), of the acid state (A) at pH 2.0 (*b*), and of the native protein (N) at pH 7.2 (*c*).
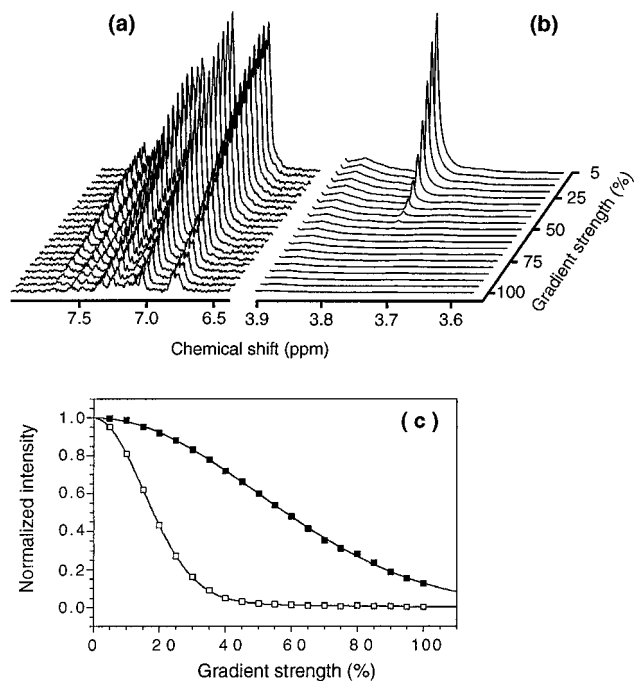
FIG. 4.   Aromatic region (*a*) and expansion of the dioxane signal (*b*) of the ^{1}H NMR spectra of the PI3-SH3 A state obtained with the PG-SLED sequence at different pulse field-gradient strengths. The signal of the small reference molecule dioxane decays much faster than the signals from the protein. (*c*) Dependence of the integral of the aromatic region between 6.6 and 7.7 ppm (■) and of the dioxane (□) signal (3.75 ppm) on the strength of the field gradient, expressed as a percentage of the maximum strength used ($\approx$60 G cm^{-1}). Data shown are derived from experiments performed on a PI3-SH3 sample (0.3 mM) at pH* 2.0 and 20°C. Analogous curves were obtained for the native protein and for the protein denatured in 3.5 M GuHCl. The solid lines in *c* correspond to fits to a Gaussian function (for the protein aromatic signals) or to a sum of two Gaussians (for the dioxane signal that resonates at a frequency where signals arising from the protein also resonate) (see ref. 26). Fitted decay rates are proportional to the diffusion coefficients for the protein and dioxane molecules, which are inversely proportional to their effective hydrodynamic radii.

measured at two different low concentrations (300 μM and 70 μM) are effectively identical; the signals in the NMR spectrum of the A state are relatively narrow, and neither the spectrum nor the line width of the A state signals shows any dependence on protein concentration between 1 mM and 70 μM.

The CD spectrum of the A state in the near-UV region is very similar to the spectrum of the denatured protein (Fig. 5*a*). Both spectra are flat and show a small, positive molar ellipticity (per aromatic residue) of 94 ± 39 degree cm^2 dmol^{-1} in the range 255–291 nm. This is in contrast to the spectrum of the native protein, which has a pronounced negative ellipticity with a minimum centered at 270 nm (−590 degree cm^2 dmol^{-1}). That the A and D states have a smaller ellipticity and a flatter spectrum than the N state indicates that the aromatic side chains in these states are in a less structured environment than in the N state. CD data in the far-UV region are in agreement with the A state being disordered as compared with the N state (Fig. 5*b*). Indeed, relative to the spectrum of the N state, the spectrum of the A state is more intense between 192 and 235 nm and exhibits a shift in the minimum of ellipticity from 204 to 200 nm, which corresponds to a CD absorption band of disordered conformations.

The N, A, and D states of PI3-SH3 were tested for ANS binding by fluorescence spectroscopy. The emission spectrum of ANS is not affected by the presence of the native protein or of the protein denatured in 3.5 M GuHCl (not shown), indicating that these do not bind ANS. The emission spectrum
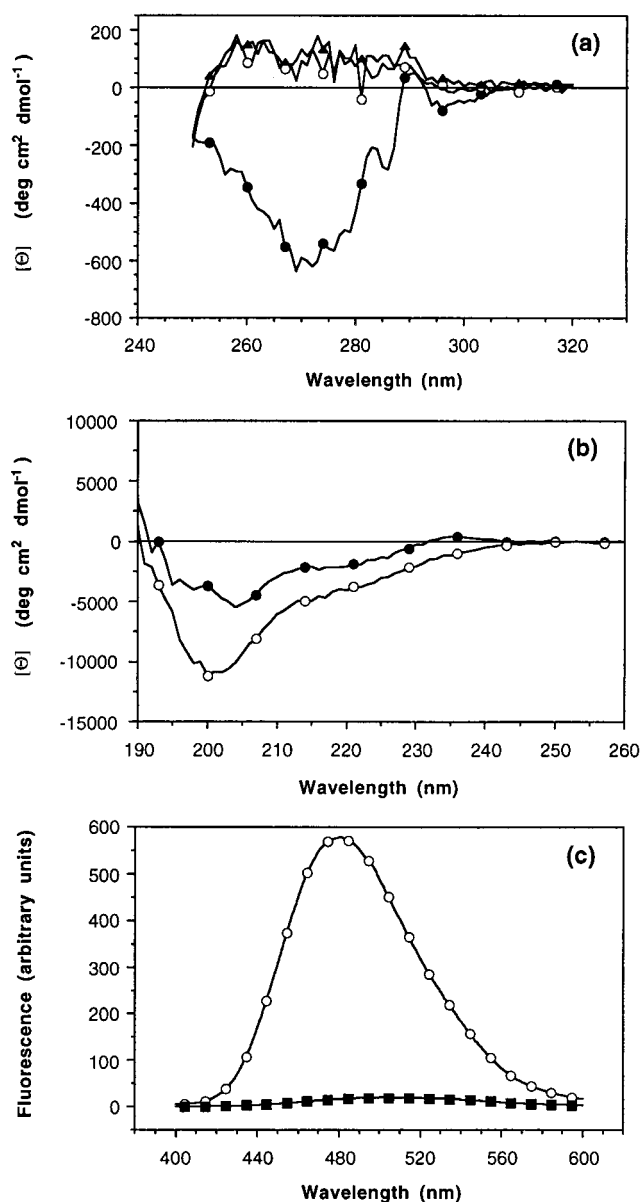

FIG. 5.   CD spectra of PI3-SH3 in the near- (*a*) and far-UV (*b*) regions (20°C). Native state, pH 7.2 (●); A state, pH 2.0 (○); and denatured state in 3.5 M GuHCl (▲). For the near-UV spectra, the ellipticity is expressed in terms of molar ellipticity per aromatic residue. Protein concentration was determined spectrophotometrically by using an extinction coefficient of 1.896 (mg/ml)$^{-1}$ cm^{-1} for the native and A states and of 2.011 (mg/ml)$^{-1}$ cm^{-1} for the denatured protein. Extinction coefficients were determined as described in ref. 32. (*c*) Fluorescence emission spectra of ANS (250 μM) in the presence of 15 μM PI3-SH3 (○) and without protein (■) acquired on pH 2.0 samples at 20°C. The excitation wavelength was 370 nm, and the excitation and emission monochromator slit widths were both set to 5 nm.

of ANS in the presence of the A state, however, shows dramatic changes (Fig. 5*c*). The A state induces a blue shift in the λ_{max} of fluorescence of ANS from 506 to 481 nm and an approximately 30-fold increase in fluorescence intensity at the corresponding maximum wavelengths. The blue shift in λ_{max} and the enhanced fluorescence of ANS caused by the A state are characteristic of ANS binding by compact, partially folded states of proteins (28, 29).

In summary, the A state of PI3-SH3 is more compact than the protein denatured in 3.5 M GuHCl but less compact than the native state, contains hydrophobic clusters that are acces-

sible to the solvent, has no extensive tertiary structure, and apparently contains little secondary structure. These characteristics indicate that, at low pH, PI3-SH3 samples an ensemble of conformations, a substantial number of which are partly folded.

CONCLUSION

We have shown that at acid pH, PI3-SH3, a small globular domain with a simple native fold, aggregates readily into amyloid fibrils. At neutral pH, PI3-SH3, which folds without accumulation of intermediates, does not form amyloid deposits (22). These results indicate that at acid pH, an amyloid-prone conformation not accessible at neutral pH is populated. The A state, as shown in this work, is a conformational ensemble of partially folded molecules. Such an ensemble will contain a dynamic distribution of structures, some of which will be highly unfolded and others of which will be highly compact (30). In the case of transthyretin (7), lysozyme (8), and the Ig light chain (9, 10), partly folded states in equilibrium with the native protein are populated under conditions favoring amyloid formation. Moreover, the effect of mutations in amyloidogenic variants of the latter three proteins is to destabilize the native protein rather than to modify the native structure, and within the range of transthyretin variants (31), there is a correlation between the thermodynamic stability and the amyloidogenicity of the variant. These data, together with the data described in this manuscript, strongly suggest that partially folded states, whether in equilibrium with unfolded or native conformers, are solution precursors to amyloid fibrils. Thus, a key issue to shed light on the molecular mechanisms of amyloid formation is the characterization of the structure of partly folded states from which amyloid deposition takes place. Further investigations are necessary to determine whether the A state of PI3-SH3 contains a high proportion of such amyloidogenic intermediates.

In this work we report a globular protein that forms amyloid fibrils but for which no amyloid-associated disease has been identified. Amyloid fibrils were found in the gel formed by PI3-SH3 without any initial hint that this gel contained amyloid. This leads us to think that amyloid formation may be a common property of globular proteins (under appropriate conditions) and that it is not a rare, exclusive property of a few proteins that are disease-associated. PI3-SH3 offers a simple model system to study amyloidogenesis, in which the native fold is known and an amyloidogenic ensemble that can be studied by techniques such as NMR has been isolated. Preliminary cryoelectron microscopy experiments of the PI3-SH3 fibrils (J. Jiménez and H. Saibil, personal communication) show a helical structure with a pitch around 580 Å and suggest that further studies might reveal ultrastructural information about amyloid fibrils. Experiments to characterize in more detail the structure of PI3-SH3 fibrils, the soluble intermediate responsible for amyloid deposition, and the mechanism of amyloid formation, are underway.

1. Tan, S. Y. & Pepys, M. B. (1994) *Histopathology* **25,** 403–414.
2. Kelly, J. W. (1996) *Curr. Op. Struct. Biol.* **6,** 11–17.
3. Sunde, M. & Blake, C. C. F. (1997) *Adv. Protein Chem.* **50,** 123–159.
4. Blake, C. & Serpell, L. C. (1996) *Structure* **4,** 989–998.
5. Sunde, M., Serpell, L. C., Bartlam, M., Fraser, P. E., Pepys, M. B. & Blake, C. C. F. (1997) *J. Mol. Biol.* **273,** 729–739.
6. Kelly, J. W. (1997) *Structure* **5,** 595–600.
7. Lai, Z., Colón, W. & Kelly, J. W. (1996) *Biochemistry* **35,** 6470–6482.
8. Booth, D. R., Sunde, M., Bellotti, V., Robinson, C. V., Hutchinson, W. L., Fraser, P. E., Hawkins, P. N., Dobson, C. M., Radford, S. E., Blake, C. C. F. & Pepys, M. B. (1997) *Nature (London)* **385,** 787–793.
9. Helms, L. R. & Wetzel, R. (1996) *J. Mol. Biol.* **257,** 77–86.
10. Wetzel, R. (1996) *Cell* **86,** 699–702.
11. Musacchio, A., Willmanns, M. & Saraste, M. (1994) *Prog. Biophys. Mol. Biol.* **61,** 283–297.
12. Morton, C. J. & Campbell, I. D. (1994) *Curr. Biol.* **4,** 615–617.
13. Booker, G. W., Gout, I., Downing, A. K., Driscoll, P. C., Boyd, J., Waterfield, M. D. & Campbell, I. D. (1993) *Cell* **73,** 813–822.
14. Koyama, S., Yu, H., Dalgarno, D. C., Shin, T. B., Zydowsky, L. D. & Schreiber, S. L. (1993) *Cell* **72,** 945–952.
15. Liang, J., Chen, J. K., Schreiber, S. L. & Clardy, J. (1996) *J. Mol. Biol.* **257,** 632–643.
16. Zhang, O. & Forman-Kay, J. D. (1995) *Biochemistry* **34,** 6784–6794.
17. Farrow, N. A., Zhang, O., Forman-Kay, J. D. & Kay, L. E. (1995) *Biochemistry* **34,** 868–878.
18. Farrow, N. A., Zhang, O. W., Forman-Kay, J. D. & Kay, L. E. (1997) *Biochemistry* **36,** 2390–2402.
19. Viguera, A. R., Martínez, J. C., Filimonov, V. V., Mateo, P. L. & Serrano, L. (1994) *Biochemistry* **33,** 2142–2150.
20. Grantcharova, V. P. & Baker, D. (1997) *Biochemistry* **36,** 15685–15692.
21. Plaxco, K. W., Guijarro, J. I., Morton, C. J., Pitkeathly, M., Campbell, I. D. & Dobson, C. M. (1998) *Biochemistry* **37,** 2529–2537.
22. Guijarro, J. I., Morton, C. J., Plaxco, K. W., Pitkeathly, M., Campbell, I. D. & Dobson, C. M. (1998) *J. Mol. Biol.* **276,** 657–667.
23. Klunk, W. E., Pettegrew, J. W. & Abraham, D. J. (1989) *J. Histochem. Cytochem.* **37,** 1293–1297.
24. Stejskal, E. O. & Tanner, J. E. (1965) *J. Chem. Phys.* **42,** 288–292.
25. Gibbs, S. J. & Johnson, C. S., Jr. (1991) *J. Magn. Reson.* **93,** 395–402.
26. Jones, J. A., Wilkins, D. K., Smith, L. J. & Dobson, C. M. (1997) *J. Biomol. NMR* **10,** 199–203.
27. Fraser, P. E., Nguyen, J. T., Surewicz, W. K. & Kirschner, D. A. (1991) *Biophys. J.* **60,** 1190–1201.
28. Semisotnov, G. V., Rodionova, N. A., Razgulyaev, O. I., Uversky, V. N., Gripas, A. F. & Gilmanshin, R. I. (1991) *Biopolymers* **31,** 119–128.
29. Chaffotte, A., Cadieux, C., Guillou, Y. & Goldberg, M. E. (1992) *Biochemistry* **31,** 4303–4308.
30. Smith, L. J., Fiebig, K. M., Schwalbe, H. & Dobson, C. M. (1996) *Fold. Des.* **1,** 95–106.
31. McCutchen, S. L., Lai, Z., Miroy, G., Kelly, J. W. & Colón, W. (1995) *Biochemistry* **34,** 13527–13536.
32. Gill, S. C. & von Hippel, P. H. (1989) *Anal. Biochem.* **182,** 319–326.